

2022

Far-Red Photography for Measuring Plant Growth: A Novel Approach

Cole Webb
Utah State University

F. Mitchell Westmoreland
Utah State University, Mitchell.Westmoreland@usu.edu

Bruce Bugbee
Utah State University, bruce.bugbee@usu.edu

Xiaojun Qi
Utah State University, xiaojun.qi@usu.edu

Follow this and additional works at: https://digitalcommons.usu.edu/cpl_techniquesinstruments

 Part of the [Agriculture Commons](#), [Computer Sciences Commons](#), and the [Plant Sciences Commons](#)

Recommended Citation

Webb, Cole; Westmoreland, F. Mitchell; Bugbee, Bruce; and Qi, Xiaojun, "Far-Red Photography for Measuring Plant Growth: A Novel Approach" (2022). *Techniques and Instruments*. Paper 20.
https://digitalcommons.usu.edu/cpl_techniquesinstruments/20

This Report is brought to you for free and open access by the Crop Physiology Lab at DigitalCommons@USU. It has been accepted for inclusion in Techniques and Instruments by an authorized administrator of DigitalCommons@USU. For more information, please contact digitalcommons@usu.edu.



Far-red photography for measuring plant growth: a novel approach

Cole Webb, F. Mitchell Westmoreland, Bruce Bugbee, Xiaojun Qi

Abstract

A critical part of agricultural studies is determining plant stress and growth rate. Modern computer vision provides a series of tools that can be applied to derive this data. In this paper, we will show our findings, analyze their accuracy, and define a system capable of deriving this data with near-human accuracy in a fraction of the time. Denoising techniques applicable to this system will be discussed, as will our discoveries and findings. Finally, suggestions for further research opportunities will be provided.

Overview

This lab has done initial work in using color imagery to separate plants from their backgrounds (Klassen et al., 2003, 3-14). This has worked in the past (Zhen & Bugbee, 2020) because plants are frequently grown in white surroundings, and software can fairly simply distinguish between white and green.

This work has included several methods, including using manual methods to segment the images and using custom software to segment color images (Johnson, 2019). These methods all have downsides, which this system aims to reduce or eliminate.

This system, however, only works well when plants are photographed under light that accurately reflects colors. Using various colors of light is common in *Cannabis* agriculture (Westmoreland et al., 2021), and therefore color accurate lighting for photography is not guaranteed.

The system described herein sidesteps this entire problem by focusing on using infrared and far-red light instead of the visible spectrum. This comes with the added advantage of high reflectance from healthy plant tissue in this spectrum, which greatly simplifies the software needed to gain high-quality results. As we will explore, this spectrum is present in trace amounts even in lights with only cool white LEDs, and those trace amounts are more than sufficient for this system to work effectively.

Methods

The vast majority of this data is gathered from images taken in a standard growth chamber. This chamber is aluminum on the inside, with a plastic grate in the bottom, and is lit from above by a pair of BIOS ICARUS Vi 321-TUXJ-00007 cool white panels. It measures 1.25m wide by 0.9m

deep by 1.02 m tall. Despite containing very little far-red light, there is enough for our purposes (as our results will show).

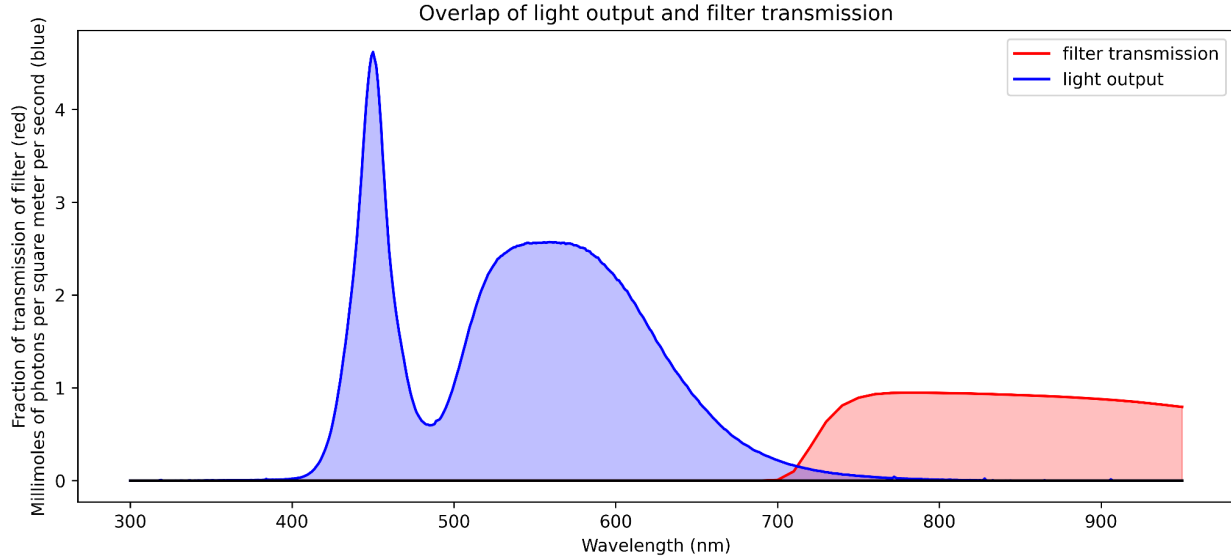


Figure 1. overlap of cool white LEDs and transmission of filter

We also did some work in a smaller chamber (0.44m wide by 0.59m deep by 1.00m tall) with less useful optical properties. This chamber was highly reflective on the inside, and the results from it were interesting but not as accurate.

The larger chamber was covered on the bottom with a sheet of black plastic, which provides a clean background to work with during the analytical process. In some studies, the plastic was augmented with a pair of crosses made of high-visibility tape. This was done to assist in lining up images taken at the same time, a process that was not pursued.

The images were taken with either a Raspberry Pi Camera Module V2, for the color images, or a Raspberry Pi NoIR Camera Module V2, for the IR images. In the case of the IR images, we placed a Schott RG9 filter in front of the lens, limiting the camera to only far-red and IR light. The camera was hooked up to a Raspberry Pi 4, which was responsible for timing the photographs and uploading them to USU's cloud storage. This was accomplished with a combination of Linux utilities and custom software.

We found that the most critical optical condition, besides having sufficient light, is contrast in brightness between the plant and its surroundings. The larger chamber, with its aluminum walls, had this property. The smaller chamber, with its painted white and highly reflective walls, did not.

Figure 2 depicts a sample infrared image. This image was taken in the larger chamber.

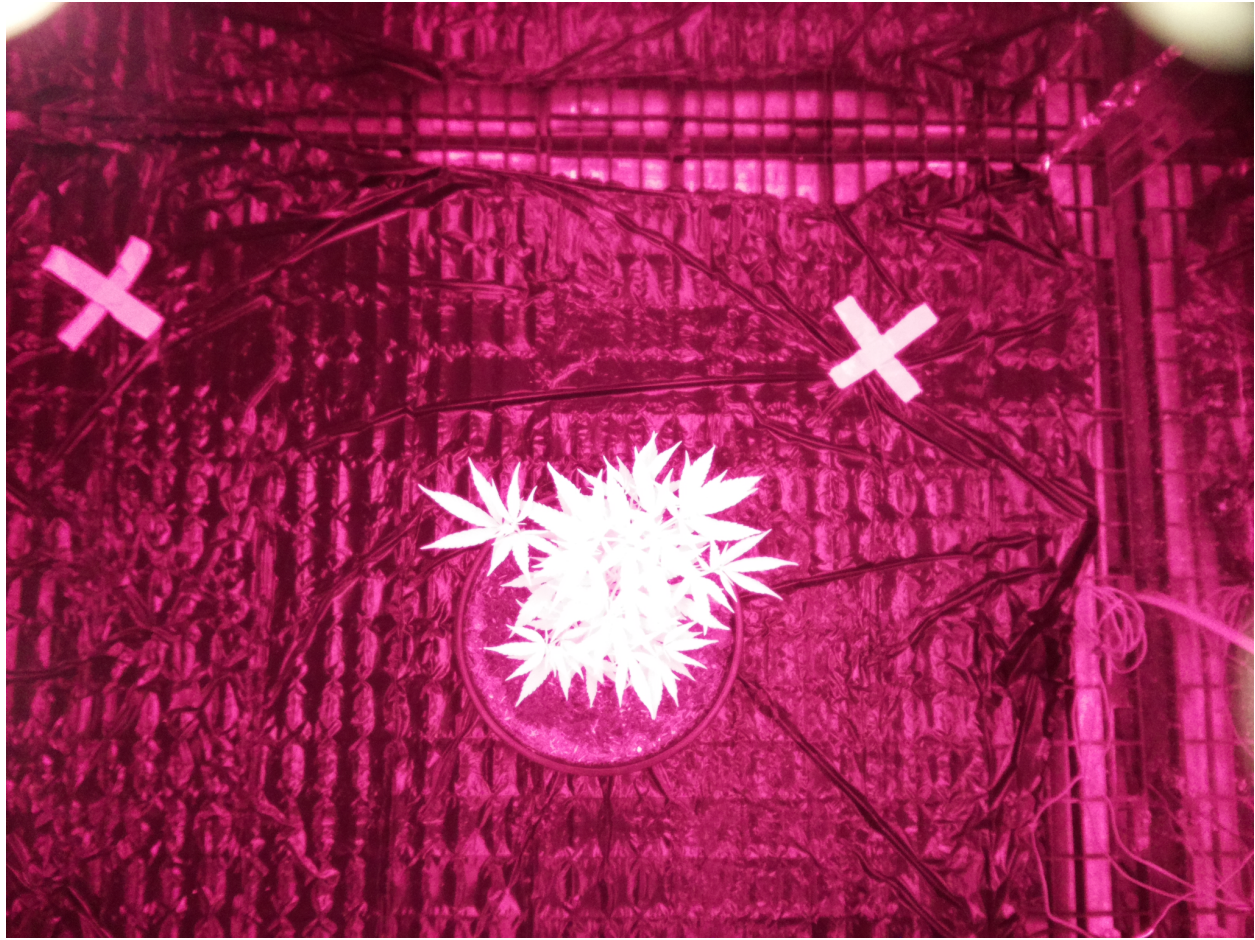


Figure 2. a sample infrared image, taken from above the plant with imaging targets

From here, the images were downloaded from cloud storage and run through the custom analytical engine. This engine contains options for a variety of denoising methods. We found the strongest correlation to time, and obtained the cleanest images, using a combination of Otsu's Binarization (Otsu) and connected component cleanup.

Otsu's Binarization looks at the histogram of a grayscale image and attempts to find a point between the two largest peaks. Anything darker than that point becomes black, anything brighter becomes white, and a grayscale image is converted to solely black and white. This algorithm has become a common tool for separating background and foreground in grayscale images, and is the default tool for image binarization in the popular scientific mathematics platform MATLAB (MathWorks, n.d.) and was therefore a natural choice for this project.

Connected component cleanup relies on the concept of connected components. A pixel is part of a connected component if it is directly or diagonally adjacent to another pixel or group of pixels of the same color. Using connected component analysis on a binary image, we can determine which pixels are in which connected components. From here, it is fairly simple to assume that the plant in the picture is the largest connected component, and delete the rest of

the connected components. We can also extend this, selecting the x largest connected components and keeping them, where x is the number of plants in the picture.

We also tried using morphological cleanup. Morphological cleanup, in this case, used two operations: an erosion operation and a dilation operation. The erosion operation shrinks the size of any object in a binary image, and the dilation image expands any object in a binary image. By combining these two operations, we get an operation called “binary closing”, which removes salt and pepper noise and thin, long extensions. While it makes large objects look blockier, it does so consistently, and therefore doesn’t affect results. While this method may be useful for other datasets, it caused minimal improvement in accuracy for this dataset.

Combining Otsu’s binarization and connected component cleanup gives us results that, under good optical conditions, are comparable to human results and significantly faster.

Finally, we counted the number of white pixels in the image and recorded them in a spreadsheet file for further analysis and plotting and saved the analyzed images for visual inspection.

Images taken while the lights were off during the night were detected by taking the mean of the grayscale image and rejecting the image from analysis if the mean was under a threshold value. We achieved 100% accuracy in this dataset using the threshold mean value of 20 (on a scale from 0 to 255).

On our test machine, analyzing a month’s worth of data took approximately 37.8 seconds. This machine consists of an 11th generation Intel i7, with 8 cores boosted to 5.5 GHz, along with a NVIDIA RTX 2070 Super. This time was achieved using a multithreaded version of the processing algorithm. The processing algorithm is processor bound, and could be further optimized by tapping into the graphics card better.

Results

Our test dataset consists of 850 images taken of a single plant over the course of 35 days. We ran the dataset through the analytical engine a total of four times, using the following settings, and calculated R^2 values to check for correlation with time.

R^2 was calculated with respect to a sigmoidal logistic curve with 4 parameters. This curve closely matches the expected behavior of a plant growth curve, with a relatively flat beginning, a period of rapid growth, and an asymptotic ending. The 4 parameters were selected by SigmaPlot for closeness of fit. Time was the independent variable, and pixel count was the dependent variable.

Run number	Otsu's Binarization?	Connected component cleanup?	Morphological cleanup?	R ²
1	Yes	No	No	0.4192
2	Yes	Yes	No	0.4980
3	Yes	No	Yes	0.4519
4	Yes	Yes	Yes	0.4991

Table 1. Summary of test runs and correlations

As we can see from Table 1, the combination of Otsu's Binarization and both denoising techniques provides the best R² value. However, the difference between using both denoising systems and using just connected component cleanup is negligible, and using morphological cleanup produces a blocky image that doesn't map cleanly to the original image. It should be noted that these R² values are artificially low, due to a lack of recorded data during the plant's night cycle. The data points from the night cycle were set to zero by convention.

We also used a set of measures from computer vision to measure accuracy: True Positive Value, False Positive Ratio, Jaccard's Index, Dice's Coefficient, and Area Error Ratio. These five measures compare the analyzed images to ground truth images, which were in this case created by manually correcting the analyzed images. We sampled images from the dataset 24 hours apart for this process.

Measure	Condition	Perfect Value	Mean Value
True Positive Ratio	Higher is better	1	0.9808
False Positive Ratio	Lower is better	0	0.001189
Jaccard's Index	Higher is better	1	0.9786
Dice's Coefficient	Higher is better	1	0.9839
Area Error Ratio	Lower is better	0	0.07124

Table 2. Summary of computer vision statistics

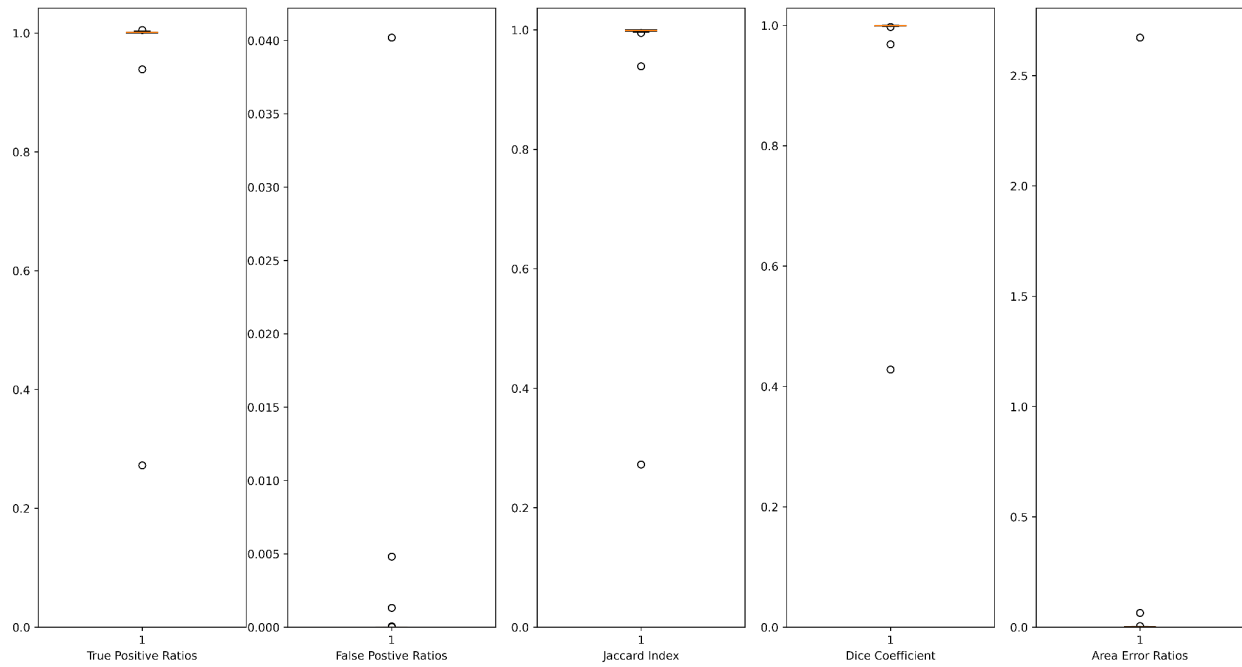


Figure 3. Box plots of computer vision statistics

Figure 3 shows whisker plots of the five computer vision statistics. Note that the scales vary. These plots show that the statistics are closely clustered around the perfect values, with several outliers.

As we can see from the above statistics and whisker plots, this algorithm performs very well. The False Positive Ratio accurately reflects that the majority of the corrections necessary added pixels to the correct images, instead of removing pixels. With the exception of an outlier, the Area Error Ratio reflects high accuracy as well.

Finally, we plotted the data output from this system. Its plot is in Figure 4, which also includes markers of waterings. Water stress accounts for a lot of the dips in the data, and it accurately reflects when the plant began to wilt.

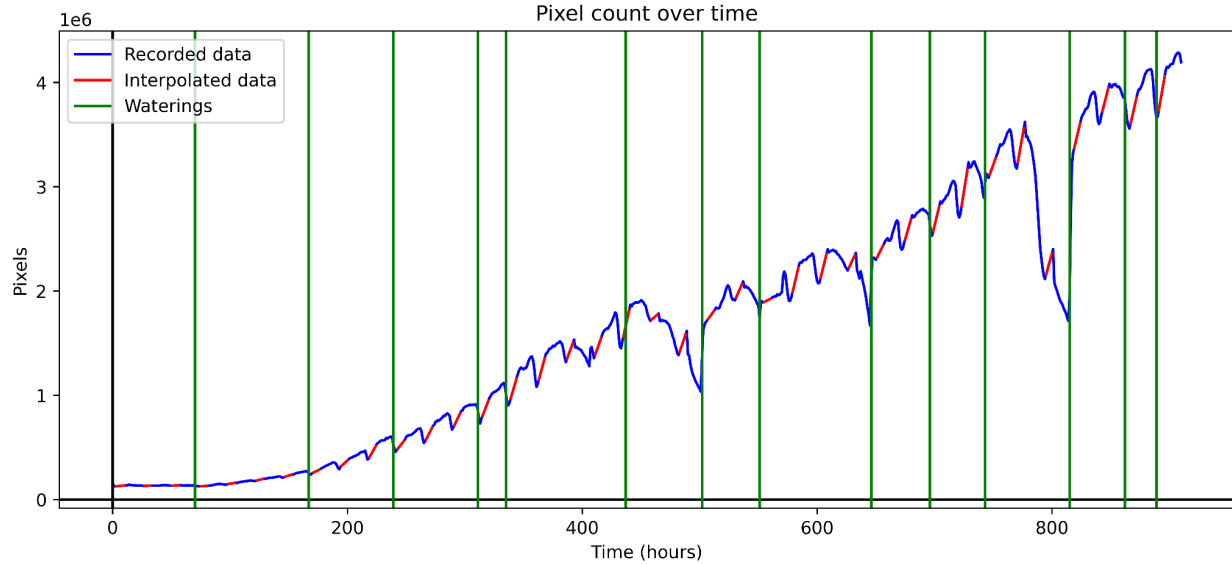


Figure 4. Output plot, including interpolated data and watering markers

The above data shows an exponential growth curve, as expected, with some considerable dips correlated to gaps in watering. The plant involved here has a circadian rhythm, which we see here as well; the plant contracts at the end of the day and is back to its usual shape by morning. Overall, the data is as expected. The system accurately detected water stress at approximately hours 510, 650, and 820. It also accurately measured the plant as it rehydrated after being watered.

This system doesn't collect data during the night, which means that we linearly extrapolated data from the night cycle. The interpolated data is marked in red on the graph above, and the recorded data from the system is marked in blue.



Figure 5. Images from a standard workflow. Original left, thresholded center, cleaned up right.

Limitations

This particular setup, with a camera at the top of the chamber looking down, only works well for plants that grow out as well as up. Grain crops, such as wheat, soybeans and corn, are not expected to work well in this system.

Further, this system relies on being able to separate a plant from its background. In order to do this, the background must be at least partially visible for the duration of the study.

This algorithm also requires that the chamber reflect less light, at least from the point of view of the camera, than the plant itself. In the smaller chamber mentioned, this was not the case; the walls of the chamber reflected almost exactly as much light as the plant, leading to the algorithm not being able to tell the difference between the plant and the walls.

Further research

The next logical step is to use this system in tandem with other ways of measuring a plant's growth rate, such as its weight or carbon dioxide consumption, and see if there is a correlation between the two figures.

Another option for exploration is building a mobile imaging system. Such an imaging system would ensure proper lighting and optical conditions for the algorithm, and make upgrades to the system simpler. It would also negate the need for in situ monitoring solutions and standardize results.

An unexpected vector for further research is an odd phenomenon we encountered while testing the system under less ideal conditions. While testing the system in the smaller chamber, for a few seconds after the lights came on in the morning, the plant appeared significantly brighter than the walls of the chamber. We have conjectured that this is chlorophyll fluorescence, but have not confirmed it. This effect gave us the contrast necessary to segment the image accurately, resulting in one clean data point per day. Previously, almost all data from this chamber had been unusable.

Finally, more accurate data could be gathered by using depth sensing hardware and software. This includes systems such as stereoscopy and time of flight sensors, which would enable us to calculate the volume of the plant instead of the area.

Conclusion

In this paper, we have shown an algorithm, combining Otsu's Binarization and connected component cleanup, that is capable of distinguishing between a plant and its surroundings. This system can also do so much faster than a human performing the same operation.

Our testbed machine ran this algorithm on the dataset in 37.8 seconds, analyzing 850 images. A human performing the same task, working fairly quickly at 5 minutes per image, would have taken over 70 hours to complete the same task. This algorithm presents a 6,746 fold improvement on the current method and as such, we believe it bears further research.

Thanks

The authors express their thanks to the entire staff of the Utah State University Crop Physiology Laboratory for their invaluable contributions to this project. Special thanks go to Brendan Fatzinger, Julie Hershkowitz, and Alec Hay.

Supplemental Material

The code for this project, in addition to Jupyter notebooks that were instrumental to the development, testing and analysis of this algorithm, can be viewed and downloaded from <https://github.com/colewebb/gpea>.

The data from this project, comprised of image data from 15 studies, can be viewed and downloaded from <https://usu.box.com/s/p1azqtuhvod9wu4wgg8p3yi2hzn806v1>.

References

- Johnson, J. (2019, February 21). *jakobottar/green-pixel-analysis: Green Pixel Counting for Plant Images*. GitHub. Retrieved April 25, 2022, from
<https://github.com/jakobottar/green-pixel-analysis>
- Klassen, S. P., Ritchie, G., Frantz, J. M., Pinnock, D., & Bugbee, B. (2003). Real-Time Imaging of Ground Cover: Relationships with Radiation Capture, Canopy Photosynthesis, and Daily Growth Rate. In T. VanToai (Ed.), *Digital Imaging and Spectral Techniques: Applications to Precision Agriculture and Crop Physiology : Proceedings of a Symposium Sponsored by Division C-2 of the Crop Science Society of America, the USDA-ARS, and the Rockefeller Foundation in Minneapolis, M* (pp. 1-14). American Society of Agronomy.
- MathWorks. (n.d.). *Global image threshold using Otsu's method - MATLAB graythresh*. MATLAB Documentation. Retrieved April 21, 2022, from
<https://www.mathworks.com/help/images/ref/graythresh.html>
- Otsu, N. (1979). A Threshold Selection Method from Gray-Level Histograms. *IEEE Transactions on Systems, Man, and Cybernetics*, 9(1), 62-66. Retrieved April 21, 2022, from
<https://ieeexplore.ieee.org/document/4310076>
- Westmoreland, F. M., Kusuma, P., & Bugbee, B. (2021, March 23). *Cannabis lighting: Decreasing blue photon fraction increases yield but efficacy is more important for cost effective production of cannabinoids*. PLoS ONE. Retrieved April 21, 2022, from
<https://journals.plos.org/plosone/article?id=10.1371/journal.pone.0248988>
- Zhen, S., & Bugbee, B. (2020, September 11). *Substituting Far-Red for Traditionally Defined Photosynthetic Photons Results in Equal Canopy Quantum Yield for CO₂ Fixation and Increased Photon Capture During Long-Term Studies: Implications for Redefining PAR*. Frontiers in Plant Science. Retrieved April 21, 2022, from
<https://www.frontiersin.org/articles/10.3389/fpls.2020.581156/full>

